potential, steep towards the Pb^{2+} ions, flat towards the unoccupied center of the elementary cell. Our investigations do not show a difference in the potentials towards the nearest F^- neighbours ($\langle 110 \rangle$ and $\langle 100 \rangle$ directions), but these potentials are clearly steeper than in the $\langle 111 \rangle$ directions towards the center of the elementary cell.

Our investigations demonstrate that elastic X-ray diffraction data allow refinements of anharmonic temperature factors up to sixth order for the Pb^{2+} ions. These temperature factors and the corresponding p.d.f. maps allow the determination of one-particle potentials, which can be used to study the thermal vibrations of the Pb^{2+} ions in arbitrary directions.

We are very indebted to Dr J. Schoonman for supplying us with crystals and to Mr B. Mühlmann for technical assistance.

References

HAMILTON, W. C. (1965). *Acta Cryst.* **18**, 502–510.
International Tables for X-ray Crystallography (1974). Vol. IV. Birmingham: Kynoch Press.
KOTO, K., SCHULZ, H. & HUGGINS, R. A. (1981). *Solid State Ionics*, **1**, 355–365.
LEHMANN, M. S. & LARSEN, F. K. (1974). *Acta Cryst.* A**30**, 580–584.
SIMMONS, G. & WANG, H. (1971). *Single Crystal Elastic Constants and Calculated Aggregate Properties – A Handbook*. London: MIT Press.
SKELTON, F. E. & KATZ, J. L. (1969). *Acta Cryst.* A**25**, 319–329.
ZUCKER, U. H., PERENTHALER, E., KUHS, W. F., BACHMANN, R. & SCHULZ, H. (1982). *PROMETHEUS*. *J. Appl. Cryst.* Submitted.
ZUCKER, U. H. & SCHULZ, H. (1982). *Acta Cryst.* A**38**, 563–568.

Acta Cryst. (1982). A**38**, 733–739

Electric Field Gradients and Charge Density in Corundum, α-Al_2O_3

BY J. LEWIS AND D. SCHWARZENBACH

Institut de Cristallographie, Université de Lausanne, Bâtiment des Sciences Physiques, 1015 *Lausanne, Switzerland*

AND H. D. FLACK

Laboratoire de Cristallographie aux Rayons X, Université de Genève, 24, *Quai Ernest Ansermet,* 1211 *Genève* 4, *Switzerland*

(*Received* 28 *December* 1981; *accepted* 6 *May* 1982)

Abstract

The charge density in α-Al_2O_3 has been refined with respect to X-ray structure factors [complete spheres for both Mo $K\alpha$ and Ag $K\alpha$ radiations with $(\sin\theta/\lambda)_{max} = 1{\cdot}19$ and $1{\cdot}495$ Å^{-1} respectively] and electric-field-gradient tensors at both atomic sites, using Hirshfeld-type deformation functions. Atomic charges from a κ refinement are $+1{\cdot}32$ (5) for Al and $-0{\cdot}88$ (8) e for O. The charge distribution of O is polarized towards the four Al neighbours, and metal–metal bonds are clearly absent. Quadrupole coupling constants and asymmetry parameters of the field-gradient tensors cannot be determined from the structure factors. They define the quadrupolar deformations near the atomic centers, and the X-ray data define the charge density between the atoms. The orientational parameters of the tensors and the signs of their largest eigenvalues can be qualitatively retrieved from the X-ray data. The refinement of anisotropic secondary-extinction parameters may, however, destroy this information. Refinement with respect to the field gradients affects mainly the quadrupolar deformation terms, and has little influence on the X-ray scale factor (*i.e.* monopolar terms) and computed electrostatic fields (*i.e.* dipolar terms). Properties of the charge density with different angular symmetries are thus only weakly correlated.

Introduction

The structure of corundum, α-Al_2O_3 (Table 3), is usually described as a hexagonal close packing of O atoms, Al occupying two thirds of the octahedral interstices. The Al substructure is analogous to rhombohedral graphite. Each AlO_6 octahedron is thus linked with three other octahedra through common edges (honeycomb net) and with one octahedron

0567-7394/82/050733-07$01.00

through a common face. As would be expected for an essentially ionic structure, the Al atoms are displaced from the octahedral centres towards the unshared faces, and shared edges are shorter than unshared edges. In fact, the two non-equivalent Al–O distances are 1·972 Å towards the shared face and 1·855 Å towards the unshared face. There are four non-equivalent O–O distances of 2·525 (shared face), 2·620 (shared edges), 2·726 (unshared edges) and 2·867 Å (unshared face). The relatively short Al–Al distance along **c** may thus be due to the particular geometrical features of the structure and not to a bonding interaction. Recently determined electron density maps in the isostructural sesquioxides Ti_2O_3 and V_2O_3 indicate the presence of different kinds of metal–metal bonds (Vincent, Yvon, Grüttner & Ashkenazi, 1980; Vincent, Yvon & Ashkenazi, 1980). These structures were not expected to be 'ionic'. The differences between the atomic distances are indeed less pronounced than in α-Al_2O_3, especially in Ti_2O_3.

Over the past few years, we have been involved in the calculation of electric field gradient tensors $\nabla\mathbf{E}$ at atomic sites from structure factors, and in the use of experimentally measured field gradients for the determination of electron density distributions (Schwarzenbach & Ngo Thong, 1979; Ngo Thong & Schwarzenbach, 1979*a*; Lewis & Schwarzenbach, 1981; Schwarzenbach & Lewis, 1982). For this purpose, corundum is a unique substance, as the complete quadrupole coupling tensors $eQ\nabla\mathbf{E}/h$ at *both* atomic sites, including their *signs*, have been measured with ^{27}Al and ^{17}O nuclear quadrupole resonance spectroscopy (NQR) using dynamic nuclear polarization (DNP) (Brun, Hundt & Niebuhr, 1968; Niebuhr, Hundt & Brun, 1968; Brun, Derighetti, Hundt & Niebuhr, 1970; Hundt, 1972). The nuclear quadrupole moments Q are +15·1 fm^2 for ^{27}Al (Endt & van der Leun, 1973) and −2·57 fm^2 for ^{17}O (Ajzenberg-Selove, 1977). The gradient at Al is characterized by *one* component ∇E_{33}(Al), the site symmetry being 3. The gradient at O with site symmetry 2 is defined by *three* terms. With the $\mathbf{e}_1$ and $\mathbf{e}_3$ axes of a local unitary coordinate system chosen along the twofold and threefold axes of the structure, these are ∇E_{11}, ∇E_{22}, $\nabla E_{33} = -(\nabla E_{11} + \nabla E_{22})$, ∇E_{23}, $\nabla E_{12} = \nabla E_{13} = 0$. The tensor is, however, more easily visualized by using its eigenvalues $\nabla E_{zz} \geq \nabla E_{yy} \geq \nabla E_{xx}$ and the orientation of the principal axes **z**, **y** and **x**. The three independent terms may then be chosen as the largest eigenvalue ∇E_{zz}(O), the asymmetry parameter $\eta(\mathrm{O}) = (\nabla E_{xx} - \nabla E_{yy})/\nabla E_{zz}$, and the angle φ(O) between **z** and **c**. The shortest principal axis **x** is parallel to the twofold axis (Table 4).

Hafner & Raymond (1968) have carried out field-gradient calculations in corundum assuming an ionic structure $Al_2^{3+}O_3^{2-}$, and taking into account the ionic dipole and quadrupole moments of O^{2-}. They succeeded in predicting η(O), φ(O) and the sign of ∇E_{zz}(O) reasonably well. The present paper describes the charge density in α-Al_2O_3 derived from X-ray diffraction and field-gradient data. A brief account of the results has been reported elsewhere (Schwarzenbach & Lewis, 1982).

Experimental

Perfectly spherical Verneuil-grown corundum crystals of various diameters were obtained from the firm Jean Sandoz SA (1470 Estavayer-le-lac, Switzerland). Their Cr content was less than 0·05%. Intensities were collected on a Syntex $P2_1$ diffractometer at room temperature, using the $2\theta:\theta$ scan technique with a θ-scan speed of 1° min^{-1}. The background intensities were determined in time sharing with data collection by an algorithm minimizing $\sigma(I)/I$ (Blessing, Coppens & Becker, 1972) modified by Schwarzenbach (1977) which permits monitoring of the reflection profiles. The intensities of *all* symmetry-equivalent reflections were measured. The stability of the instrument was monitored by measuring six symmetry-equivalent reference reflections at intervals of 50 regular measurements. The variance of an intensity was computed according to $\sigma^2(I) = \sigma^2(\text{statistics}) + (KI)^2$, where K was obtained from this formula by analyzing the fluctuations of the check reflections about their mean. For the variance of the unweighted mean value $\bar{I}$ of a set of n equivalent intensities I_i, the larger of the two quantities $\sigma_1^2(\bar{I}) = \sum \sigma^2(I_i)/n^2$ and $\sigma_2^2(\bar{I}) = \sum (I_i - \bar{I})^2/n(n-1)$ was chosen. The e.s.d.'s of the structure factors were then derived by applying the law of propagation of errors modified for small intensities. Weights used in the structure refinements with respect to $|F|$ and $|F|^2$ were $\sigma^{-2}(|F|)$ and $\sigma^{-2}(|F|^2)$, respectively. Absorption-weighted mean path lengths were taken from Flack & Vincent (1978). The free-atom scattering factors in analytical form and the dispersion corrections were taken from *International Tables for X-ray Crystallography* (1974).

Two independent data sets were collected as shown in Table 1. The internal consistency of equivalent reflections was generally excellent, except for the

Table 1. *Data collection: symbols are defined in the text*

	Data set I	Data set II
Crystal diameter (mm)	0·20	0·13
Radiation	Mo $K\alpha$ Nb-filtered	Ag $K\alpha$ Pd-filtered
Wavelength (Å)	0·71069	0·56083
$(\sin\theta/\lambda)_{max}$ (Å^{-1})	1·19	1·495
Number of reflections	4402	8923
Number of unique reflections	397	804
Unique reflections $I < 3\sigma$	10	186
Reflections with $\sigma_2 > 2\sigma_1$	15	9
K	0·006	0·008
μ (mm^{-1})	13·335	6·991
μR	1·334	0·454

strongest low-order reflections which showed pronounced anisotropic secondary extinction effects. In data set II, the ratio σ/I was generally about three times larger than in I, but extinction was smaller.*

Charge density refinements

(i) Initial structure refinements with respect to the averaged structure factors $|F|$ were carried out with a modified version of *CRYLSQ* of the XRAY system (1972). An isotropic extinction correction (Zachariasen, 1967) was included. Convergence was reached at $R(|F|) = 0.012$ and 0.017 for the observed reflections ($I > 3\sigma$) of I and II respectively (goodness of fit, GOF = 5.3 and 2.4). A very notable discrepancy of 29% occurred for the reflection 006 where $|F_o| = 16.8$ e and $F_c = 12f(\text{Al})\cos 12\pi z(\text{Al}) - 18f(\text{O}) = 9.102\ f(\text{Al}) - 18f(\text{O}) = -11.9$ e (the f's include temperature factors). This is a direct consequence of atomic charges, O being in fact negative and Al positive. In fact, a κ refinement (Coppens, Guru Row, Leung, Stevens, Becker & Yang, 1979) effectively removed the discrepancy. The charges obtained with data set II are +1.32 (5) for Al and −0.88 (8) e for O, the corresponding expansion factors κ of the valence shells are 1.20 (6) and 0.945 (4). The results for data set I are +1.24 (5), −0.83 (7) e, 1.09 (5) and 0.954 (4) respectively. κ refinements of $AlPO_4$ and SiO_2 (Ngo Thong & Schwarzenbach, 1979*a*,*b*) indicated similar charges of about +1.2 e for the metal atoms.

(ii) Charge density refinements were carried out with *LSEXP* (Hirshfeld, 1977), modified according to Schwarzenbach & Ngo Thong (1979) and Lewis & Schwarzenbach (1981). Secondary extinction parameters (Becker & Coppens, 1974, 1975) were adjusted together with all other parameters. It was found that extinction was best described as Lorentzian type I (mosaic spread dominated) with the Thornley & Nelmes (1974) form for the angular distribution. The refinements were carried out with respect to $|F|^2$, no weak reflections being excluded. All independent parameters of the deformation functions from $n = 0$ to $n = 4$ were refined, resulting in 32 population parameters and two exponents α of the radial functions $r^n \exp(-\alpha r)$. For each data set, six refinements were carried out (Table 2). An isotropic extinction correction was applied to the averaged symmetry-independent $|F|^2$ values (*a*,*b*,*c*), *or alternatively* an anisotropic extinction correction was applied to the full data sets (*d*,*e*,*f*). In *a* and *d*, the spherical-atom model was refined; in *b* and *e*, the charge density was refined against $|F|^2$ values only and the field gradients at Al and O were then calculated; in *c* and *f* the refinement was carried out simultaneously with respect to $|F|^2$ and the experimentally determined field-gradient-tensor elements. Weights chosen for the latter were σ^{-2}, with $\sigma = 3$ EV m^{-2}. The standard structural parameters from these refinements agree well with maximum deviations of 1.5 e.s.d.'s for z(Al) and x(O), and 5 e.s.d.'s for the temperature factors. Table 3 shows the results for refinement *f*2 varying the maximum number of parameters with respect to the largest data set. The computed and observed field gradients are reported in Table 4. The gradients in the spherical-atom model $\nabla\mathbf{E}$(overlap) (Schwarzenbach & Ngo Thong, 1979) were evaluated by summing the contributions of neighbouring atoms to a maximum distance of 10 Å.

* Lists of structure factors and deformation parameters have been deposited with the British Library Lending Division as Supplementary Publication No. SUP 36904 (12 pp.). Copies may be obtained through The Executive Secretary, International Union of Crystallography, 5 Abbey Square, Chester CH1 2HU, England.

Table 2. *Reliability factors, scale factors and radial exponents*

Definitions: $\text{GOF}(|F|^2) = \{\sum \text{weight} \times (|F_o|^2 - |F_c|^2)^2/(n-m)\}^{1/2} \simeq \text{GOF}(|F|)$, n = number of observations, m = number of variable parameters; $R(|F|) = \sum |F_o - F_c| / \sum F_o|$; $R_w(|F|^2) = \{\sum \text{weight} \times (|F_o|^2 - |F_c|^2)^2 / \sum \text{weight} \times |F_o|^4\}^{1/2} \simeq 2R_w(|F|)$; the sums in R and R_w include only reflections with $I > 3\sigma$; the scale factor is defined by $F_o = \text{scale} \times y \times F_{\text{corr}} = \text{scale} \times F_c$, y being the extinction correction. Refinements *a* and *d* are with respect to the spherical-atom model, secondary extinction is refined isotropically against average $|F|^2$ values in *a*, *b*, *c*, and anisotropically against the full data sets in *d*, *e*, *f*.

	∇E	GOF($\|F\|^2$)	$R(\|F\|)$	$R_w(\|F\|^2)$	$n-m$	Scale	α (Al)	α (O)
Data set I								
*a*1	—	4.92	0.012	0.027	387	9.76 (1)		
*b*1	no	2.90	0.009	0.015	353	9.9 (1)	5.6 (4)	5.2 (6)
*c*1	yes	3.01	0.010	0.016	357	9.8 (1)	5.6 (7)	7.9 (4)
*d*1	—	6.44	0.019	0.085	4387	9.96 (2)		
*e*1	no	5.98	0.018	0.079	4353	10.7 (1)	6.9 (5)	9.0 (5)
*f*1	yes	6.00	0.018	0.079	4357	10.8 (1)	7.1 (5)	8.6 (4)
Data set II								
*a*2	—	2.22	0.017	0.022	794	2.891 (4)		
*b*2	no	1.21	0.013	0.018	760	2.94 (1)	4.5 (1)	5.7 (4)
*c*2	yes	1.26	0.014	0.018	764	2.93 (1)	4.7 (2)	7.2 (3)
*d*2	—	1.44	0.044	0.056	8908	3.008 (2)		
*e*2	no	1.13	0.042	0.044	8874	3.05 (1)	4.2 (1)	4.2 (1)
*f*2	yes	1.14	0.042	0.044	8878	3.03 (1)	4.4 (1)	7.0 (2)

Table 3. *Structural parameters obtained with refinement f2*

The temperature-factor expression is exp $\{-2\pi^2 \sum h_i h_j a_i^* a_j^* U_{ij}\}$.

Formula	α-Al_2O_3	Extinction parameters (×10 $^{-4}$)	
a (Å)	4·7602 (4)	Z_{11}	11·7 (7)
c (Å)	12·9933 (17)	Z_{22}	5·7 (3)
V (Å^3)	254·98 (5)	Z_{33}	1·8 (1)
Number of units	6	Z_{12}	−5·9 (4)
F(000)	300	Z_{13}	−0·1 (2)
Space group	$R\bar{3}c$	Z_{23}	0·6 (1)
12Al in (c)	0 0 z(Al)		
z(Al)	0·35216 (1)	Al—O (Å)	1·8551 (2), 1·9716 (3)
U_{11} (Å^2)	0·00279 (3)	O—O (Å)	2·5249 (3), 2·6200 (3)
U_{33} (Å^2)	0·00296 (3)		2·7255 (3), 2·8665 (3)
18O in (e)	x(O) 0 $\frac{1}{4}$		
x(O)	0·30624 (4)		
U_{11} (Å^2)	0·00327 (3)		
U_{22} (Å^2)	0·00341 (3)		
U_{33} (Å^2)	0·00365 (3)		
U_{13} (Å^2)	0·00047 (2)		

Table 4. *Observed and calculated field gradients in* α-Al_2O_3

Units of ∇E are 10^2 EV m^{-2}, e.s.d.'s are given in parentheses. ∇E_{33}(Al) is the gradient along **c**. The principal axes **x**,**y**,**z** of the observed gradient at O are defined by $|\nabla E_{xx}| \leq |\nabla E_{yy}| \leq |\nabla E_{zz}|$, $0 \leq \eta(\mathrm{O}) \leq 1$; **x** is parallel to the **a** axis for O at x(O) 0 $\frac{1}{4}$. The corresponding principal axes of the computed tensors are labelled as the nearest principal axes of the observed tensor, and *not* according to their eigenvalues. φ(O) is the angle between **z** and **c**, $\varphi(\mathrm{O}) = +90°$ for **z** parallel to **b***.

	Extinction	∇E_{33}(Al)	∇E_{zz}(O)	η(O)	φ(O)
$b1$	iso	−3·9 (5·4)	+12·0 (3·6)	0·3 (0·4)	41 (7)
$e1$	aniso	+23·1 (8·1)	+52·2 (6·0)	−0·3 (0·2)	21 (5)
$b2$	iso	−24·0 (3·0)	+11·7 (3·0)	0·2 (0·4)	44 (6)
$e2$	aniso	+2·4 (2·1)	+6·0 (1·2)	1·5 (0·4)	28 (4)
Observed		−6·553	+34·872	0·517	45·85

In data set II, the scale factor increased on the average by 3·7% in going from isotropic to anisotropic extinction. In data set I, however, it increased by 10% for refinements $e1$ and $f1$. Concomitantly, the extinction parameters Z_{ij} decreased with respect to refinement $d1$ and the radial exponents α increased. The more narrow mosaic distribution and the smaller absolute intensities lead to nearly unchanged extinction corrections y. The largest correlation coefficients between scale factor, extinction parameters, population parameters of $n = 0$ functions and α's ranged from 0·7 to 0·8, whereas for data set II they were below 0·65. The scale factor obtained in $e1$ and $f1$ is clearly too high, as evidenced by the corresponding deformation maps (not reproduced here) which show deep troughs at both atomic positions. A similar effect has been found in Li_3N (Lewis & Schwarzenbach, 1981). In fact, the monopolar $n = 0$ functions are able to simulate the scattering of the core electrons at large sin θ/λ, and the low-order intensities can be described adequately by adjusting the deformation and extinction parameters. The more extensive data set II alleviates this problem, and the scale is only a function of the extinction formalism used. The extinction tensors Z_{ij} obtained with the two data sets, *i.e.* with two crystals coming from the same source, differ by at most 4 e.s.d.'s. The principal axes of the mosaic distribution are aligned approximately along **c**, **b*** and **a** with half widths of 4, 6 and 11″. The extinction correction $y_{\min}$ for the strongest reflection $30\bar{3}0$ is near 0·76 for all refinements $a1$ to $f1$, and near 0·85 for $a2$ to $f2$. Using the field gradients as observations led to slightly less anisotropic tensors and improved the convergence of the least-squares calculations.

Static model maps were obtained by Fourier summations of the structure factors calculated with the deformation functions only. They have thus the same resolution as the data. Those resulting from data set II are shown in Figs. 1–5. The corresponding maps from refinements $b1$ and $c1$ agree well with Figs. 1 and 2, but the latter have much smoother contours (Schwarzenbach & Lewis, 1982). The maps from $e1$ and $f1$ clearly show the incorrect monopolar properties mentioned above. The e.s.d.'s of the deformation densities were estimated with *DEFSYN* (Hirshfeld, 1977) by sum-

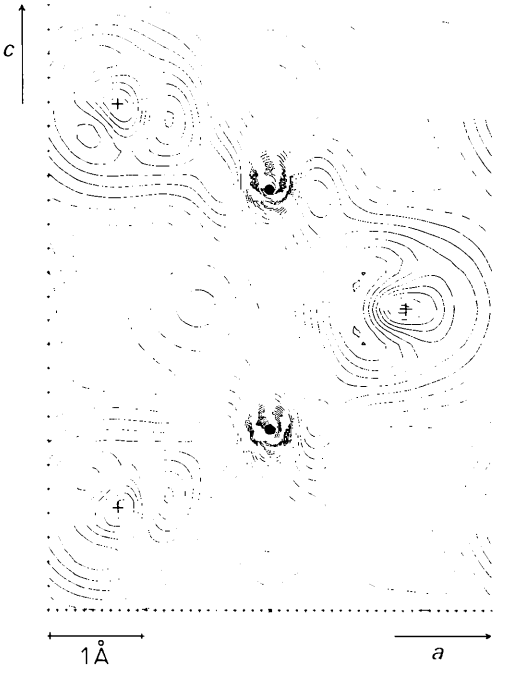

Fig. 1. Static model deformation map of α-Al_2O_3 in the plane $(01\bar{1}0)$ through two Al and three O atoms, the terminal ones deviating from the plane by 0·12 Å. The face shared by two AlO_6 octahedra passes through the central O and is perpendicular to the plot. The octahedra, *i.e.* the Al atoms, are related by a diad axis. Refinement $b2$, interval 0·05 e Å^{-3}, negative contours broken. E.s.d.'s are 0·02 e Å^{-3} between Al and O, and 0·03 e Å^{-3} between Al and Al. They increase to 0·1 e Å^{-3} at distances of 0·33 and 0·23 Å from the sites of Al and O, respectively.

ming up the variances and covariances of the deformation parameters for each grid point.

Results and discussion

The most frequently published field-gradient data are quadrupole coupling constants and asymmetry parameters. Precisely these quantities, ∇E_{33}(Al), ∇E_{zz}(O) and η(O), cannot be derived from our structure factors, their e.s.d.'s being very large (Table 4). The sign at O on the other hand is always correctly obtained. In addition, the refinements using isotropic extinction yield also the correct sign at Al, the correct angle φ(O) and the correct order of the eigenvalues at O with respect to their absolute size, *i.e.* $0 < \eta(O) < 1$. Thus, the orientational parameters can be qualitatively retrieved from the X-ray data, as predicted by Stewart (1976). None of this information, excepting the sign at O, is found in the refinements using anisotropic extinction. There, the gradient at Al has the wrong sign, φ(O) is too small, and the order of the eigenvalues is incorrect, i.e. $\eta(O) < 0$ in *e*1 and >1 in *e*2. The quadrupolar deformation functions are correlated with the second-order extinction tensor in much the same way as the monopolar functions are correlated with the scale factor. The particular orientation of the very anisotropic extinction tensor with one eigenvector along **c** appears to be responsible for the wrong sign at Al, since the mean extinction correction of a set of equivalent intensities depends on the angle between the reciprocal-lattice vector and **c**. The quadrupolar deformation functions at Al have cylindrical symmetry, **c** being the unique axis. Their scattering factors depend on the same angle.

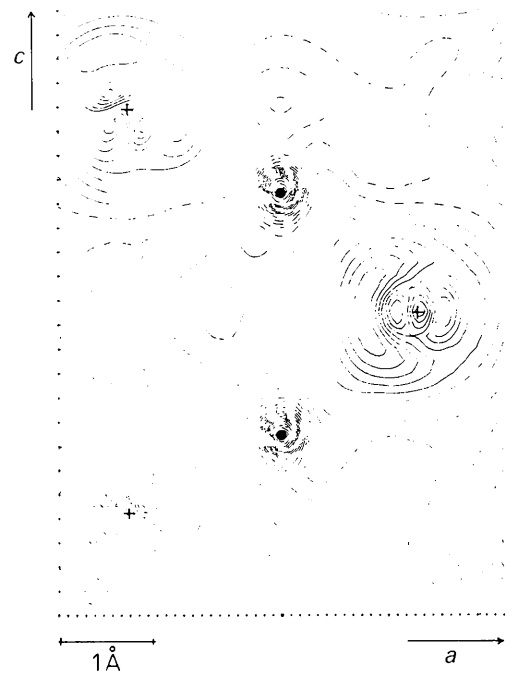

Fig. 2. As Fig. 1 for refinement *c*2. The centre of O is a peak flanked by two troughs.

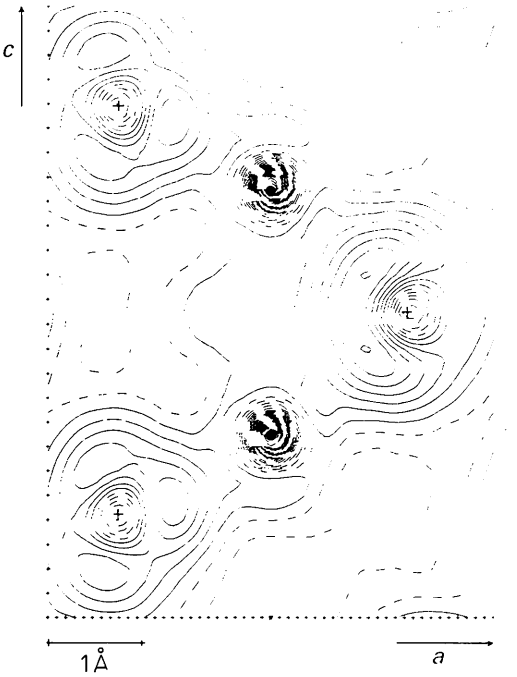

Fig. 3. As Fig. 1 for refinement *e*2. E.s.d.'s are 0·01 e Å^{-3} between Al and O, as well as between Al and Al. They increase to 0·1 e Å^{-3} at distances of 0·26 and 0·17 Å from the sites of Al and O, respectively.

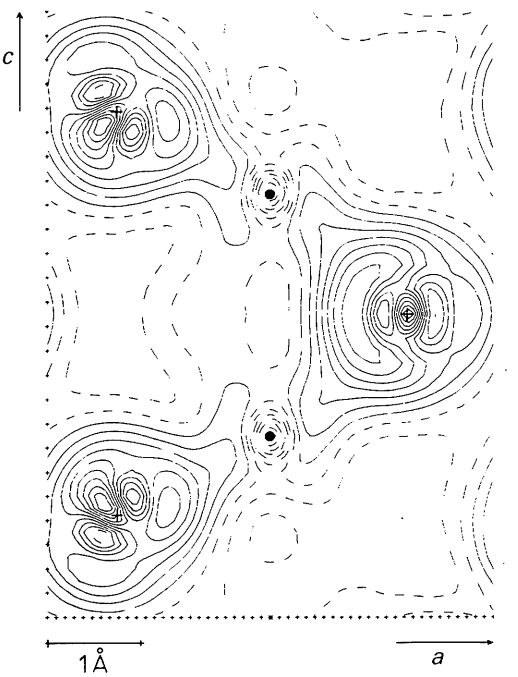

Fig. 4. As Fig. 1 for refinement *f*2. E.s.d.'s are as in Fig. 3.

Refinements *e*1 and *f*1 show again (Lewis & Schwarzenbach, 1981) that a refinement with respect to field gradients cannot improve the X-ray scale factor. Computed field gradients hardly depend on the assumed scale factor. Computed electrostatic fields at the atomic sites are typically −42 (12) and −30 (9) GV m^{-1} along the triad axis at Al and the diad axis at O respectively. The zero-field condition of the Hellmann–Feynman electrostatic theorem is thus obeyed within 3·5 e.s.d.'s. Since these values are similar in *all* refinements, we conclude that *properties* of the charge density with different angular symmetries are only weakly correlated, in agreement with Stewart (1977).

The overall features of Figs. 1–4 agree well. They show an important charge migration from Al to O, and there are electron density bridges along the Al–O bonds. The short bond pointing towards the unshared octahedral face is similar to the long bond pointing towards the shared face. Fig. 5 shows a section through these faces. There are no density maxima between the metal atoms, either along **c** as in Ti_2O_3 (Vincent, Yvon, Grüttner & Ashkenazi, 1980), or perpendicular to **c** as in V_2O_3 [Vincent, Yvon & Ashkenazi (1980); the density in the $(11\bar{2}0)$ plane is not reproduced here since it presents no features of interest in corundum]. Although this may not, by itself, rule out metal–metal bonds (Martin, Rees & Mitschler, 1982), the comparison with the other sesquioxides indicates that they are negligible. The differences between Figs. 1–4 are found near the atomic centres. The refinements with respect to the X-ray data alone yield troughs at all atomic positions which are deeper in Fig. 3 than in Fig. 1, as would be expected from the larger scale factor implied by the anisotropic extinction correction. Using the field gradients as observations virtually eliminates the negative regions at O which are replaced by two troughs separated by positive electron density. This feature may not represent the true charge density, but it *does* possess the correct quadrupolar properties.

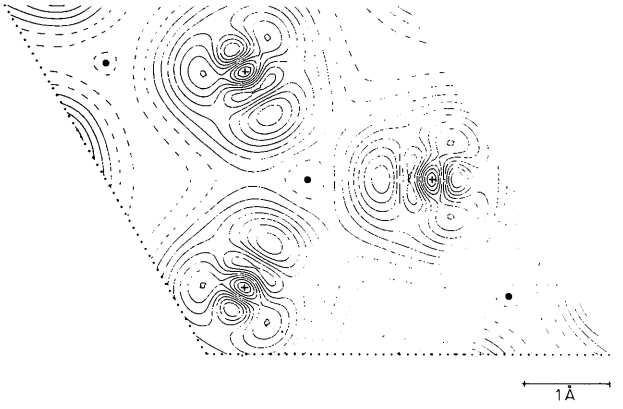

Fig. 5. Static model deformation map in the plane (0001), through the centres of the O atoms. The centre of the plot is a shared octahedral face, flanked by two unshared faces. Refinement *f*2. Al (●) is located above and/or below the section.

The close similarity of Fig. 4 with Fig. 2 is most striking. It appears that the anisotropic extinction formalism is unnecessary if the field gradients are used as observations and the quadrupolar properties are thus imposed on the charge density. Judging from Fig. 3 and the field gradients computed from both data sets, the much simpler anisotropic correction is even to be preferred in refinements against X-ray data only. This is a surprising result since the extinction is definitely anisotropic. Note, however, that the averaged structure factors have been obtained from a full sphere of data. A partial data set does not give satisfactory results, neither in an isotropic nor in an anisotropic extinction refinement. It also appears to be important to refine deformation and extinction parameters together, particularly in the anisotropic case, since even a small change of the extinction tensor may have a noticeable effect on the deformation density. The necessity of evaluating extinction with the free-atom model can be one of the drawbacks of the usual *X–N* and *X–X* syntheses.

We thank Professor E. Brun, University of Zürich, for the NQR data. The calculations were carried out at the computer center of the Swiss Federal Institute of Technology at Lausanne (CDC Cyber NOS/BE). The project is supported by the Swiss National Science Foundation, grants 2.234–0.79 and 2.067–0.81.

References

AJZENBERG-SELOVE, F. (1977). *Nucl. Phys. A*, **281**, 1–148.

BECKER, P. J. & COPPENS, P. (1974). *Acta Cryst.* A**30**, 129–153.

BECKER, P. J. & COPPENS, P. (1975). *Acta Cryst.* A**31**, 417–425.

BLESSING, R. H., COPPENS, P. & BECKER, P. J. (1972). *J. Appl. Cryst.* **7**, 488–492.

BRUN, E., DERIGHETTI, B., HUNDT, E. E. & NIEBUHR, H. H. (1970). *Phys. Lett.* **31**A, 416–417

BRUN, E., HUNDT, E. & NIEBUHR, H. (1968). *Helv. Phys. Acta*, **41**, 417.

COPPENS, P., GURU ROW, T. N., LEUNG, P., STEVENS, E. D., BECKER, P. J. & YANG, Y. W. (1979). *Acta Cryst.* A**35**, 63–72.

ENDT, P. M. & VAN DER LEUN, C. (1973). *Nucl. Phys. A*, **214**, 1–625.

FLACK, H. D. & VINCENT, M. G. (1978). *Acta Cryst.* A**34**, 489–491.

HAFNER, S. & RAYMOND, M. (1968). *J. Chem. Phys.* **49**, 3570–3579.

HIRSHFELD, F. L. (1977). *Isr. J. Chem.* **16**, 226–229.

HUNDT, E. (1972). *Kernresonanz von* ^{17}O *und* ^{27}Al *in Rubin: Kopplungsparameter und Relaxation.* PhD Thesis, Philosophische Fakultät II, Univ. of Zürich, Switzerland.

International Tables for X-ray Crystallography (1974). Vol. IV. Birmingham: Kynoch Press.

LEWIS, J. & SCHWARZENBACH, D. (1981). *Acta Cryst.* A**37**, 507–510.

MARTIN, M., REES, B. & MITSCHLER, A. (1982). *Acta Cryst.* B**38**, 6–15.
NGO THONG & SCHWARZENBACH, D. (1979*a*). *Acta Cryst.* A**35**, 658–664.
NGO THONG & SCHWARZENBACH, D. (1979*b*). Collected Abstracts Fifth European Crystallogr. Meet., p. 348.
NIEBUHR, H. H., HUNDT, E. E. & BRUN, E. (1968). *Phys. Rev. Lett.* **21**, 1735–1738.
SCHWARZENBACH, D. (1977). Collected Abstracts Fourth European Crystallogr. Meet., PI 20.
SCHWARZENBACH, D. & LEWIS, J. (1982). *Electron Distributions and the Chemical Bond*, edited by M. B. HALL & P. COPPENS. New York: Plenum Press. In the press.
SCHWARZENBACH, D. & NGO THONG (1979). *Acta Cryst.* A**35**, 652–658.
STEWART, R. F. (1976). *Acta Cryst.* A**32**, 565–574.
STEWART, R. F. (1977). *Isr. J. Chem.* **16**, 124–131.
THORNLEY, F. R. & NELMES, R. J. (1974). *Acta Cryst.* A**30**, 748–757.
VINCENT, M. G., YVON, K. & ASHKENAZI, J. (1980). *Acta Cryst.* A**36**, 808–813.
VINCENT, M. G., YVON, K., GRÜTTNER, A. & ASHKENAZI, J. (1980). *Acta Cryst.* A**36**, 803–808.
XRAY system (1972). Tech. Rep. TR-192. Computer Science Center, Univ. of Maryland, College Park, Maryland. Implemented and extended by D. Schwarzenbach.
ZACHARIASEN, W. H. (1967). *Acta Cryst.* **23**, 558–564.

Short Communications

Contributions intended for publication under this heading should be expressly so marked; they should not exceed about 1000 *words; they should be forwarded in the usual way to the appropriate Co-editor; they will be published as speedily as possible.*

Acta Cryst. (1982). A**38**, 739–740

A comment on the method of determination of the polarization ratio for crystal-monochromated X-rays by Vincent & Flack.

By A. MCL. MATHIESON, *CSIRO, Division of Chemical Physics, PO Box* 160, *Clayton, Victoria, Australia* 3168

(*Received* 17 *September* 1981; *accepted* 26 *March* 1982)

Abstract

By reference to previously unpublished tests, the validity of the experimental procedure proposed by Vincent & Flack [*Acta Cryst.* (1980), A**36**, 614–620] for the measurement of the polarization factor is questioned.

Introduction

In a recent group of papers (Vincent & Flack, 1980*a*,*b*; Flack & Vincent, 1980), aspects of the polarization ratio for crystal-monochromated X-rays have been treated. A method of determining this ratio was proposed (Vincent & Flack, 1980*b*) which involved two series of measurements, one with a β filter and the other with a monochromator crystal. The numerical results reported appear to differ significantly from others recorded in the literature.

Comments arising from experimental work of a similar type, carried out in 1972 but not previously reported, are offered.

Procedure

The procedure used was based on use of a number of low-intensity reflexions of α-glycine ($C_2H_5NO_2$), with 2θ values selected to span the effective range of the diffractometer (Picker). Choice of the low-intensity reflexions was to avoid or at least minimize the effects of extinction [a naive viewpoint held at the time of the experiment but subsequently modified (Mathieson, 1979)]. Measurements were carried out using Cu $K\alpha$ radiation (*a*) with a β filter and (*b*) with a pyrolytic graphite crystal mounted on a device (Mathieson, 1968) which allowed ready change from one configuration to the other. The change involved lowering the scintillation counter, removing the monochromator crystal and inserting the β filter. Being a post-monochromator arrangement (see Mathieson, 1968), the basic components of the experiment, the glycine crystal and the diffractometer, were presumed not affected in any way.

To test the effectiveness of the procedure, a graphical presentation was preferred. This was based on the following; for the monochromator in the perpendicular position, Fig. 1, with counter azimuth, $\varphi = 90°$ (see Mathieson, 1968), the diffracted intensity is proportional to $k + \cos^2 2\theta$ where k is the polarization ratio of the monochromator crystal, while with the β filter it is proportional to $1 + \cos^2 2\theta$. The ratio of intensity with the monochromator to that with the β filter, $R_{m/\beta}$, is therefore given by

$$R_{m/\beta} \propto (k + \cos^2 2\theta)/(1 + \cos^2 2\theta). \quad (1)$$

This can be rearranged:

$$R_{m/\beta} \propto (k - 1)(1 + \cos^2 2\theta)^{-1} + 1, \quad (2)$$

0567-7394/82/050739-02$01.00